Double-diffusive natural convection in a differentially heated wavy cavity under thermophoresis effect

Teodor Groşan[1]

Babeş-Bolyai University, 400084 Cluj-Napoca, Romania

Mikhail A. Sheremet[2,3]

Tomsk State University, 634050, Tomsk, Russia

Tomsk Polytechnic University, 634050, Tomsk, Russia

Ioan Pop[4*]

Babeş-Bolyai University, 400084 Cluj-Napoca, Romania

Serban Rareş Pop[5]

University of Chester, CH1 4BJ Chester, UK

Abstract

A numerical analysis is made for thermophoretic transport of small particles through the convection in a differentially heated square cavity with a wavy wall. The governing gas-particle partial differential equations are solved numerically for some values of the considered parameters to investigate their influence on the flow, heat and mass transfer patterns. It is found that the effect of thermophoresis can

[1] Associate Professor, Department of Mathematics
[2,3] Professor, Laboratory on Convective Heat and Mass Transfer, Department of Nuclear and Thermal Power Plants
[4*] Professor, Department of Mathematics, ipop@math.ubbcluj.ro (correspondent author)
[5] Senior Lecturer, Department of Computer Sciences

be quite significant in appropriate situations. The number of undualtions can essentially modify the heat transfer rate and fluid flow intensity.

Nomenclature

Roman letters

C_1, C_2 = concentrations

C = aerosol particle concentration

d_p = particle diameter

$\mathbf{g}$ = gravitational acceleration vector

k_p = thermal conductivity of aerosol particle

k_T = dimensionless coefficient

Kn = Knusen number

L = length and height of the cavity

$\mathbf{n}$ = vector normal to the wavy surface

N_C, N_T = thermophoresis parameters

Nu = local Nusselt number

$\overline{Nu}$ = average Nusselt number

p = pressure

Pr = Prandtl number

Ra = Rayleigh number

Sc = Schmidt number

Sh = local Sherwood number

$\overline{Sh}$ = average Sherwood number

t = dimensional time

T = dimensional temperature

T_C = low temperature

T_h = high temperature

$u,\ v$ = dimensionless velocity components

$\overline{u},\ \overline{v}$ = dimensional velocity components

$\overline{u}_T,\ \overline{v}_T$ = thermophoretic deposition velocity components

x, y = dimensionless Cartesian coordinates

$\overline{x},\ \overline{y}$ = dimensional Cartesian coordinates

Greek symbols

α = thermal conductivity

β = buoyancy ratio parameter

β_T = volumetric thermal expension coefficient

β_C = volumetric diffusion expension coefficient

ϕ = nanoparticles volume fraction

κ = number of undulations

λ = gas mean free path)

μ = dynamic viscosity

ν = kinematic viscosity

θ = dimensionless temperature

ρ = density

τ = dimensionless time

σ = surface of the wavy cavity

ξ, η = new independent variables

ω = dimensionless vorticity

ψ = dimensionless stream function

Keywords: Free convection; Wavy wall; Differentially heated cavity; Thermophoresis effect; Numerical results

I. Introduction

THE effect of thermophoresis known as a temperature gradient induces an opposite movement to low-sized gas suspended particles, has been studied considerable in the past and has many industrial applications such as: air-cleaning devices to remove submicron- and micron-sized particles from gas streams, deposition of particulate material on heat exchanger surfaces (Epstain et al. [1]), problems including nuclear reactor safety (Tsai and Liang [2]), modified chemical vapor deposition (Jenson et al. [3]), in the semiconductor industry (Opiolka et al. [4]), optical fiber fabrication (Song and Hwang [5]), etc. In the presence of a temperature gradient, in addition to other forces like drag, gravity or Brownian, a thermophoretic force depending on Knudsen number acts on the aerosol particles. Reviews of theory and experiments done in the field can be found in Bakarov [6], He and Ahmadi [7], and Piazza and Parola [8]. Thermophoretic aerosol particles deposition in the boundary layer flow of a Newtonian fluid has been extensively studied. Epstein et al. [1] have studied the thermophoretic deposition in a natural convection boundary layer on a cold vertical plate. Goren [9] investigated the thermophoretic deposition in a laminar compressible boundary layer flow past a flat plate. Wang and Chen [10] studied the deposition of particles from a boundary layer flow onto a continuously moving wavy surface, etc. They found that the particle concentration at the wall has very close values in both laminar and turbulent flow and that the particles are attracted by a plate colder than the gas and the concentration drops monotonically as the wall is approached. The thermophoretic aerosol particles deposition in a

fluid-saturated porous media was studied by Chamkha and Pop [11] for a vertical flat plate and Postelnicu [12] for a horizontal flat plate. They reported a high deposition of particles on the plate which increases when the thermophoresis parameter increases.

With many industrial and environmental applications, the natural convection of enclosed fluids has been an important subject due to its particular transition to turbulence mechanism by destabilizing the buoyancy-driven flow and its high numerical computational requirements. A large section of the previous research done on this topic has been reviewed by Bejan [13]. Extensive work was done by De Vahl Davis [14] who presented the final form of the problem and computational results for high Rayleigh numbers. The complexity of the system is increased when the convective is not only driven by temperature but concentration differences also. Beghein et al. [15] investigated numerically the thermosolutal natural convection in a square cavity filled with air mixed with different kinds of pollutants subject to horizontal temperature and concentration gradients. Sheremet [16] has investigated the effects of Soret and Dufour effects on heat transfer and fluid flow patterns in a square cavity with and without solid walls. An essential influence of contaminant source on flow and heat transfer structure has been shown. Sezai and Mohamad [17] have studied the double-diffusive convection in a cubic enclosure with opposing temperature and concentration gradients. The results showed a significant influence of solutal buoyancy force and Lewis number on heat and mass transfer rate at high values of Rayleigh numbers. Kuznetsov and Sheremet [18, 19] have examined numerically double-diffusive natural convection in a square [18] and cubical [19] cavities bounded by solid walls of finite thickness and conductivity with a local heat and contaminant sources. It has been revealed the effect of buoyancy ratio parameter on intensification of heat and mass transfer process.

In general, the main assumption of the studies which considered the free and mixed convection flow in vertical channels is that the thermophoretic deposition of aerosol particles is negligible. However, due to its fundamental and technological importance, theoretical studies of the thermophoretic effects on particle deposition in channel, tube or pipe flow were performed by many

investigators (Weinberg [20], Fiebig et al. [21], Grosan et al. [22], Chang et al. [23]), etc. Moreover, Chein and Liao [24] presented a numerical model including both the particle molecular diffusion and thermophoretic effects to study nanoparticle deposition in a two-dimensional channel flow subject to two types of thermal conditions. Talbot et al. [25] analyzed the thermophoresis of particles in a heated boundary layer, and Batchelor and Shen [26] studied the thermophoretic deposition in a gas flow over a cold surface. Many practical and industrial applications of the thermophoretic effects can be found in the open literature, for example, a method for hybridization and binding between biomolecules involving thermophoresis, the thermophoretic filtering of liquids and the process for preparation of ceramic film are mentioned in the patents ([27] and [28]).

Wavy shaped enclosures are used in engineering applications as given by Varol and Oztop [29], Sultana and Hyder [30], Shenoy et al. [31], etc. Circular, square and an arc-square cavity whose shape lies between the square and circular cavity are analyzed by Ridouane and Campo [32]. They used finite volume method and found that the heat transfer enhancement provided by the circular cavity is large for low Rayleigh numbers and decreases for moderate Rayleigh number and practically vanishes for higher values of Rayleigh number. We mention also here the very interesting papers by Siddiqa et al. [33,34] on dynamics of two-phase dusty fluid flow along a wavy surface and on double diffusive natural convection flow over a wavy surface situated in a non-absorbing medium.

Based on above literature survey, the number of studies on double-diffusive natural convection in a differentially heated wavy cavity under thermophoresis effect is still limited especially for curvilinear surfaces. To the authors' best knowledge, the thermophoretic transport effects in the steady convective flow in a wavy cavity have not been studied before and it is the main aim of this paper to study this problem. The scope of this paper is to numerically analyze the effect of thermophoresis on natural convection in a differentially heated square cavity having a wavy wall filled with a Newtonian fluid containing suspended aerosol particles. Streamlines, isotherms, isoconcentration contours as well as average Nusselt number and fluid flow rate are presented and discussed in details.

II. Basic equations

We analyze the free convective flow and heat transfer of a warm gas, containing suspended aerosol particles, inside a differentially heated square cavity with a wavy isothermal wall. The domain of interest is presented in Fig. 1 with dimensional Cartesian coordinate system where the origin is set in the cavity's bottom left corner, the $\overline{x}$-axis is a horizontal axis and $\overline{y}$-axis is a vertical axis with opposite direction relative to the gravitational acceleration. The considered enclosure is kept at constant temperatures T_1 and T_2 and constant concentrations C_1 and C_2 at the left wavy and right flat walls, while horizontal walls are adiabatic and impermeable. The length and height of the cavity is denoted by L. It is assumed that the left wavy wall and right flat wall of the cavity are described by the following relations $\overline{x}_1 = L - L\left[a + b\cos(2\pi\kappa\overline{y}/L)\right]$ and $\overline{x}_2 = L$, respectively. $\overline{\Delta} = \overline{x}_2 - \overline{x}_1 = L\left[a + b\cos(2\pi\kappa\overline{y}/L)\right]$ is the distance between vertical walls.

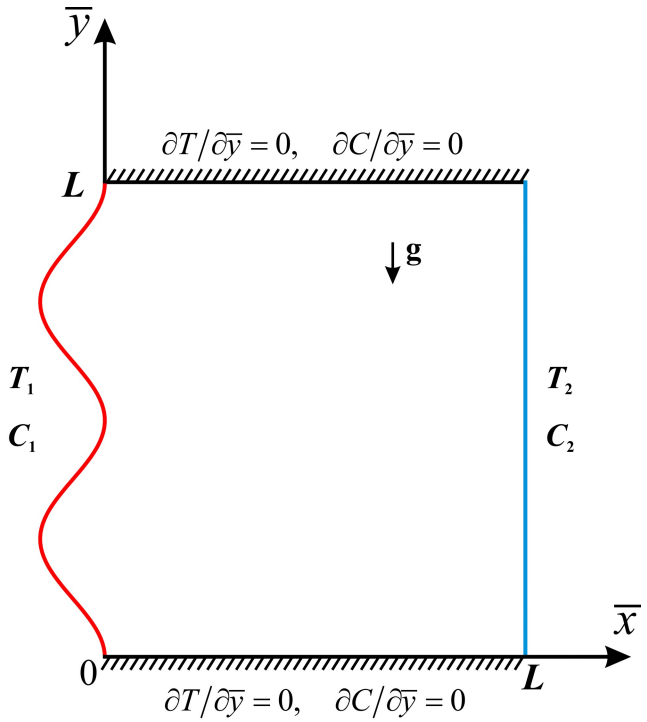

Fig. 1. Physical model and coordinate system

Except for the density, the properties of the fluid are taken to be constant. It is further assumed that the effect of buoyancy is included through the Boussinesq approximation in the following form:

$$\rho = \rho_0 \left[1 - \beta_T (T - T_c) - \beta_C (C - C_c) \right] \tag{1}$$

The viscous, radiation and Joule heating effects are neglected. Under the above assumptions, the conservation equations for mass, momentum and thermal energy can be written in Cartesian coordinates as follows:

$$\frac{\partial \overline{u}}{\partial \overline{x}} + \frac{\partial \overline{v}}{\partial \overline{y}} = 0 \tag{2}$$

$$\rho \left(\frac{\partial \overline{u}}{\partial t} + \overline{u} \frac{\partial \overline{u}}{\partial \overline{x}} + \overline{v} \frac{\partial \overline{u}}{\partial \overline{y}} \right) = - \frac{\partial p}{\partial \overline{x}} + \mu \left(\frac{\partial^2 \overline{u}}{\partial \overline{x}^2} + \frac{\partial^2 \overline{u}}{\partial \overline{y}^2} \right) \tag{3}$$

$$\rho \left(\frac{\partial \overline{v}}{\partial t} + \overline{u} \frac{\partial \overline{v}}{\partial \overline{x}} + \overline{v} \frac{\partial \overline{v}}{\partial \overline{y}} \right) = - \frac{\partial p}{\partial \overline{y}} + \mu \left(\frac{\partial^2 \overline{v}}{\partial \overline{x}^2} + \frac{\partial^2 \overline{v}}{\partial \overline{y}^2} \right) + \rho \left[\beta_T (T - T_c) + \beta_C (C - C_c) \right] g \tag{4}$$

$$\frac{\partial T}{\partial t} + \overline{u} \frac{\partial T}{\partial \overline{x}} + \overline{v} \frac{\partial T}{\partial \overline{y}} = \alpha \left(\frac{\partial^2 T}{\partial \overline{x}^2} + \frac{\partial^2 T}{\partial \overline{y}^2} \right) \tag{5}$$

$$\frac{\partial C}{\partial t} + \overline{u} \frac{\partial C}{\partial \overline{x}} + \overline{v} \frac{\partial C}{\partial \overline{y}} + \frac{\partial (\overline{u}_T C)}{\partial \overline{x}} + \frac{\partial (\overline{v}_T C)}{\partial \overline{y}} = D \left(\frac{\partial^2 C}{\partial \overline{x}^2} + \frac{\partial^2 C}{\partial \overline{y}^2} \right) \tag{6}$$

Here $(\overline{u}, \overline{v})$ are the dimensional velocity components along the Cartesian coordinates $(\overline{x}, \overline{y})$, T is the fluid temperature, C is a aerosol particle concentration, $\overline{u}_T$ and $\overline{v}_T$ are the thermophoretic deposition velocity components, which are defined as

$$\overline{u}_T = - k_T \frac{\nu}{T} \frac{\partial T}{\partial \overline{x}}, \quad \overline{v}_T = - k_T \frac{\nu}{T} \frac{\partial T}{\partial \overline{y}} \tag{7}$$

and the physical meaning of the other quantities is mentioned in the nomenclature. The dimensionless coefficient k_T depends on the Knudsen number Kn ($Kn = 2\lambda / d_p$, where d_p is the particle diameter

and λ is the gas mean free path) and the ratio of the thermal conductivity between the gas and particles. According to Talbot et al. [25], k_T is expressed as

$$k_T = \frac{2.34 \cdot \eta \left[k_f / k_p + 2.18 \cdot Kn \right]}{(1 + 3.42 \cdot Kn)(1 + 2\, k_f / k_p + 4.36 \cdot Kn)} \tag{8}$$

The values of k_T is in the range between 0.2 and 1.2 (Batchelor and Shen [26]), k_f is a thermal conductivity of fluid, k_p is a thermal conductivity of aerosol particles, η is a Cunningham correction factor. Further, it is assumed that particles have only one size, hence the particulate matter is diluted enough that pairs or groups of particles may be considered (Epstein et al. [1]).

In order to analyze the fluid flow and heat transfer in general scale we introduce the following dimensionless variables

$$\begin{aligned} &\tau = t\sqrt{g\beta_T (T_h - T_c) L}/L,\ x = \bar{x}/L,\ y = \bar{y}/L,\ u = \bar{u}/\sqrt{g\beta_T (T - T_c) L}, \\ &v = \bar{v}/\sqrt{g\beta_T (T - T_c) L},\ \theta = (T - T_c)/(T_h - T_c),\ \phi = (C - C_c)/(C_h - C_c) \end{aligned} \tag{9}$$

and also dimensionless stream function $\psi \left(u = \frac{\partial \psi}{\partial y},\ v = -\frac{\partial \psi}{\partial x} \right)$ and vorticity $\omega = \frac{\partial v}{\partial x} - \frac{\partial u}{\partial y}$. Therefore the governing Eqs. (2)–(6) using the dimensionless variables (9) can be written as follows

$$\frac{\partial^2 \psi}{\partial x^2} + \frac{\partial^2 \psi}{\partial y^2} = -\omega \tag{10}$$

$$\frac{\partial \omega}{\partial \tau} + u\frac{\partial \omega}{\partial x} + v\frac{\partial \omega}{\partial y} = \sqrt{\frac{Pr}{Ra}}\nabla^2 \omega + \frac{\partial \theta}{\partial x} + \beta \frac{\partial \phi}{\partial x} \tag{11}$$

$$\frac{\partial \theta}{\partial \tau} + \frac{\partial \psi}{\partial y}\frac{\partial \theta}{\partial x} - \frac{\partial \psi}{\partial x}\frac{\partial \theta}{\partial y} = \frac{1}{\sqrt{Ra \cdot Pr}}\left(\frac{\partial^2 \theta}{\partial x^2} + \frac{\partial^2 \theta}{\partial y^2} \right) \tag{12}$$

$$\begin{aligned} &\frac{\partial \phi}{\partial \tau} + \frac{\partial \psi}{\partial y}\frac{\partial \phi}{\partial x} - \frac{\partial \psi}{\partial x}\frac{\partial \phi}{\partial y} = \frac{1}{Sc}\sqrt{\frac{Pr}{Ra}}\left(\frac{\partial^2 \phi}{\partial x^2} + \frac{\partial^2 \phi}{\partial y^2} \right) + \\ &+ k_T \sqrt{\frac{Pr}{Ra}} \left\{ \frac{\partial}{\partial x}\left(\frac{\phi + N_C}{\theta + N_T} \cdot \frac{\partial \theta}{\partial x} \right) + \frac{\partial}{\partial y}\left(\frac{\phi + N_C}{\theta + N_T} \cdot \frac{\partial \theta}{\partial y} \right) \right\} \end{aligned} \tag{13}$$

with the following boundary conditions

$$\begin{aligned}
&\psi = 0, \quad \omega = -\frac{\partial^2 \psi}{\partial x^2} - \frac{\partial^2 \psi}{\partial y^2}, \quad \theta = 1, \quad \phi = 1 \quad \text{on the left wavy wall} \\
&\psi = 0, \quad \omega = -\frac{\partial^2 \psi}{\partial x^2}, \quad \theta = 0, \quad \phi = 0 \quad \text{on the right flat wall} \\
&\psi = 0, \quad \omega = -\frac{\partial^2 \psi}{\partial y^2}, \quad \frac{\partial \theta}{\partial y} = 0, \quad \frac{\partial \phi}{\partial y} = 0 \quad \text{on the bottom and top walls}
\end{aligned} \tag{14}$$

Here $Ra = g\beta_T \Delta T L^3 / (\nu\alpha)$ is the Rayleigh number, $Pr = \nu/\alpha$ is the Prandtl number, $\beta = \frac{\beta_C \Delta C}{\beta_T \Delta T}$ is the buoyancy ratio parameter, $Sc = \nu/D$ is the Schmidt number, $N_C = \frac{C_c}{\Delta C}$ and $N_T = \frac{T_c}{\Delta T}$ are the thermophoresis parameters, $\Delta C = C_h - C_c$ and $\Delta T = T_h - T_c$.

It is interesting to note that when $\beta = 0$ there is no mass transfer and the buoyancy force is due to thermal diffusion only. The mass transfer driven flow is valid for both positive and negative values of β. Hence, the two buoyant mechanisms aid each other when $\beta > 0$ and oppose each other when $\beta < 0$, respectively (Mahajan and Angirasa [35]).

The physical quantities of interest are the local Nusselt number Nu and local Sherwood number along the hot wavy wall and average Nusselt number $\overline{Nu}$ and average Sherwood number $\overline{Sh}$, that are defined as

$$\begin{aligned}
Nu &= -\left.\frac{\partial \theta}{\partial \mathbf{n}}\right|_{x=0}, \quad \overline{Nu} = \int_0^1 Nu \, dy \\
Sh &= -\left.\frac{\partial \phi}{\partial \mathbf{n}}\right|_{x=0}, \quad \overline{Sh} = \int_0^1 Sh \, dy
\end{aligned} \tag{15}$$

III. Numerical method

The cavity in the x and y plane, i.e., physical domain, is transformed into a rectangular geometry in the computational domain using an algebraic coordinate transformation by introducing new independent variables ξ and η. The left and right walls of the cavity become coordinate lines having constant values of ξ. The independent variables in the physical domain are transformed to independent variables in the computational domain by the following equations:

$$\begin{cases} \xi = \dfrac{x - x_1}{\Delta} = \dfrac{x - 1 + a + b \cdot \cos(2\pi\kappa y)}{a + b \cdot \cos(2\pi\kappa y)}, \\ \eta = y \end{cases} \tag{16}$$

Taking into account transformation (16) the governing equations (10)–(13) will be rewritten in the following form:

$$\left[\left(\frac{\partial \xi}{\partial x} \right)^2 + \left(\frac{\partial \xi}{\partial y} \right)^2 \right] \frac{\partial^2 \psi}{\partial \xi^2} + 2 \frac{\partial \xi}{\partial y} \frac{\partial^2 \psi}{\partial \xi \partial \eta} + \frac{\partial^2 \psi}{\partial \eta^2} + \frac{\partial^2 \xi}{\partial y^2} \frac{\partial \psi}{\partial \xi} = -\omega \tag{17}$$

$$\begin{aligned} &\frac{\partial \omega}{\partial \tau} + \frac{\partial \xi}{\partial x} \frac{\partial \psi}{\partial \eta} \frac{\partial \omega}{\partial \xi} - \frac{\partial \xi}{\partial x} \frac{\partial \psi}{\partial \xi} \frac{\partial \omega}{\partial \eta} = \sqrt{\frac{Pr}{Ra}} \left\{ \left[\left(\frac{\partial \xi}{\partial x} \right)^2 + \left(\frac{\partial \xi}{\partial y} \right)^2 \right] \frac{\partial^2 \omega}{\partial \xi^2} + \right. \\ &\left. + 2 \frac{\partial \xi}{\partial y} \frac{\partial^2 \omega}{\partial \xi \partial \eta} + \frac{\partial^2 \omega}{\partial \eta^2} + \frac{\partial^2 \xi}{\partial y^2} \frac{\partial \omega}{\partial \xi} \right\} + \frac{\partial \xi}{\partial x} \frac{\partial \theta}{\partial \xi} + \beta \frac{\partial \xi}{\partial x} \frac{\partial \phi}{\partial \xi} \end{aligned} \tag{18}$$

$$\frac{\partial \theta}{\partial \tau} + \frac{\partial \xi}{\partial x} \frac{\partial \psi}{\partial \eta} \frac{\partial \theta}{\partial \xi} - \frac{\partial \xi}{\partial x} \frac{\partial \psi}{\partial \xi} \frac{\partial \theta}{\partial \eta} = \frac{1}{\sqrt{Ra \cdot Pr}} \left\{ \left[\left(\frac{\partial \xi}{\partial x} \right)^2 + \left(\frac{\partial \xi}{\partial y} \right)^2 \right] \frac{\partial^2 \theta}{\partial \xi^2} + 2 \frac{\partial \xi}{\partial y} \frac{\partial^2 \theta}{\partial \xi \partial \eta} + \frac{\partial^2 \theta}{\partial \eta^2} + \frac{\partial^2 \xi}{\partial y^2} \frac{\partial \theta}{\partial \xi} \right\} \tag{19}$$

$$\begin{aligned} &\frac{\partial \phi}{\partial \tau} + \frac{\partial \xi}{\partial x} \frac{\partial \psi}{\partial \eta} \frac{\partial \phi}{\partial \xi} - \frac{\partial \xi}{\partial x} \frac{\partial \psi}{\partial \xi} \frac{\partial \phi}{\partial \eta} = \frac{1}{Sc} \sqrt{\frac{Pr}{Ra}} \left\{ \left[\left(\frac{\partial \xi}{\partial x} \right)^2 + \left(\frac{\partial \xi}{\partial y} \right)^2 \right] \frac{\partial^2 \phi}{\partial \xi^2} + 2 \frac{\partial \xi}{\partial y} \frac{\partial^2 \phi}{\partial \xi \partial \eta} + \frac{\partial^2 \phi}{\partial \eta^2} + \frac{\partial^2 \xi}{\partial y^2} \frac{\partial \phi}{\partial \xi} \right\} + \\ &+ k_T \sqrt{\frac{Pr}{Ra}} \left\{ \left(\frac{\partial \xi}{\partial x} \right)^2 \frac{\partial}{\partial \xi} \left(\frac{\phi + N_C}{\theta + N_T} \cdot \frac{\partial \theta}{\partial \xi} \right) + \frac{\partial \xi}{\partial y} \frac{\partial}{\partial \xi} \left[\frac{\phi + N_C}{\theta + N_T} \cdot \left(\frac{\partial \xi}{\partial y} \frac{\partial \theta}{\partial \xi} + \frac{\partial \theta}{\partial \eta} \right) \right] + \frac{\partial}{\partial \eta} \left[\frac{\phi + N_C}{\theta + N_T} \cdot \left(\frac{\partial \xi}{\partial y} \frac{\partial \theta}{\partial \xi} + \frac{\partial \theta}{\partial \eta} \right) \right] \right\} \end{aligned}$$

(20)

The corresponding boundary conditions are given by

$$\psi = 0, \quad \omega = -\left[\left(\frac{\partial \xi}{\partial x}\right)^2 + \left(\frac{\partial \xi}{\partial y}\right)^2\right]\frac{\partial^2 \psi}{\partial \xi^2} - 2\frac{\partial \xi}{\partial y}\frac{\partial^2 \psi}{\partial \xi \partial \eta} - \frac{\partial^2 \xi}{\partial y^2}\frac{\partial \psi}{\partial \xi}, \quad \theta = \frac{T_1 - T_c}{T_h - T_c}, \quad \phi = \frac{C_1 - C_c}{C_h - C_c} \quad \text{on } \xi = 0$$

$$\psi = 0, \quad \omega = -\left(\frac{\partial \xi}{\partial x}\right)^2 \frac{\partial^2 \psi}{\partial \xi^2}, \quad \theta = \frac{T_2 - T_c}{T_h - T_c}, \quad \phi = \frac{C_2 - C_c}{C_h - C_c} \quad \text{on } \xi = 1$$

$$\psi = 0, \quad \omega = -\frac{\partial^2 \psi}{\partial \eta^2}, \quad \frac{\partial \theta}{\partial \eta} = 0, \quad \frac{\partial \phi}{\partial \eta} = 0 \quad \text{on } \eta = 0 \text{ and } \eta = 1$$

(21)

Here

$$\frac{\partial \xi}{\partial x} = \frac{1}{a + b\cos(2\pi\kappa y)}, \quad \frac{\partial \xi}{\partial y} = \frac{2\pi\kappa b(x-1)\sin(2\pi\kappa y)}{\left[a + b\cos(2\pi\kappa y)\right]^2}, \quad \frac{\partial^2 \xi}{\partial x^2} = 0$$

$$\frac{\partial^2 \xi}{\partial y^2} = \frac{4\pi^2\kappa^2 b(x-1)\sin\left[a\cos(2\pi\kappa y) + b + b\sin^2(2\pi\kappa y)\right]}{\left[a + b\cos(2\pi\kappa y)\right]^3}$$

(22)

The local Nusselt number along the left wavy wall can be found as follows:

$$Nu = -\left(\frac{\partial \theta}{\partial \mathbf{n}}\right)_{x=x_1} = -(\mathbf{n}, \nabla\theta)_{\left\{\mathbf{n} = -\frac{1}{\sqrt{1+\sigma_y^2}}\mathbf{i} + \frac{\sigma_y}{\sqrt{1+\sigma_y^2}}\mathbf{j}\right\}} = \frac{1}{\sqrt{1+\sigma_y^2}}\left.\frac{\partial \theta}{\partial x}\right|_{x=x_1} - \frac{\sigma_y}{\sqrt{1+\sigma_y^2}}\left.\frac{\partial \theta}{\partial y}\right|_{x=x_1} \tag{23}$$

or taking into account Eq. (16) we can obtain

$$Nu = \frac{1}{\sqrt{1+\sigma_y^2}}\left(\frac{\partial \xi}{\partial x} - \sigma_y \left.\frac{\partial \xi}{\partial y}\right|_{x=x_1}\right)\left.\frac{\partial \theta}{\partial \xi}\right|_{\xi=0} \tag{24}$$

The local Sherwood number also can be defined as

$$Sh = \frac{1}{\sqrt{1+\sigma_y^2}}\left(\frac{\partial \xi}{\partial x} - \sigma_y \left.\frac{\partial \xi}{\partial y}\right|_{x=x_1}\right)\left.\frac{\partial \phi}{\partial \xi}\right|_{\xi=0} \tag{25}$$

Therefore, the average Nusselt and Sherwood numbers can be defined as

$$\overline{Nu} = \int_0^1 Nu\, d\eta, \quad \overline{Sh} = \int_0^1 Sh\, d\eta. \tag{26}$$

The governing equations (17)–(20) with corresponding boundary conditions (21) were solved using the finite difference method of the second order accuracy (see Sheremet [16], Kuznetsov and Sheremet [18, 19], Shenoy et al. [31]). Comprehensive description and verification of the used numerical schemes have been presented earlier (see Sheremet [16], Kuznetsov and Sheremet [18, 19], Shenoy et al. [31]).

The developed in-house computational code has been verified using numerical data by Sezai and Mohamad [17] for the double-diffusive convection in a square cavity, filled with a binary fluid such as an aqueous solution. Different temperatures and concentrations are specified between the left and right vertical walls and zero heat and mass fluxes are imposed on the remaining walls with no slip boundary conditions for all velocity components. The flow is assumed to be laminar and the binary fluid is assumed to be Newtonian and incompressible. The comparison of results is analyzed in terms of the average Nusselt and Sherwood numbers (see Table 1).

Table 1. Variations of $\overline{Nu}$ and $\overline{Sh}$ with Ra for $Pr = Le = 10$, $\beta = -0.5$

Ra	Sezai and Mohamad [17]		Present data	
	$\overline{Nu}$	$\overline{Sh}$	$\overline{Nu}$	$\overline{Sh}$
10^2	1.0	1.0	1.0	1.0
10^3	1.07	2.5	1.09	2.45
10^4	2.21	5.28	2.18	5.29
$5 \cdot 10^4$	3.64	–	3.65	8.94
10^5	4.5	–	4.53	11.29

For the purpose of obtaining grid independent solution, a grid sensitivity analysis is performed. The grid independent solution was performed by preparing the solution for free convection in a square wavy cavity filled with a warm gas, containing suspended aerosol particles at $Ra = 10^4$, $Pr = 0.7$, $Sc = 10.0$, $\beta = 1.0$, $N_T = 8$, $N_C = 2$, $k_T = 1.0$, $\kappa = 2$, $a = 0.9$, $T_1 = T_h$, $T_2 = T_c$, $C_1 = C_c$, $C_2 = C_h$. Four cases of the uniform grid are tested: a grid of 50×50 points, a grid of 100×100 points, a grid of 150×150

points, and a much finer grid of 200×200 points. Figure 2 shows an effect of the mesh parameters on the average Nusselt number of the left wavy wall and fluid flow rate inside the cavity.

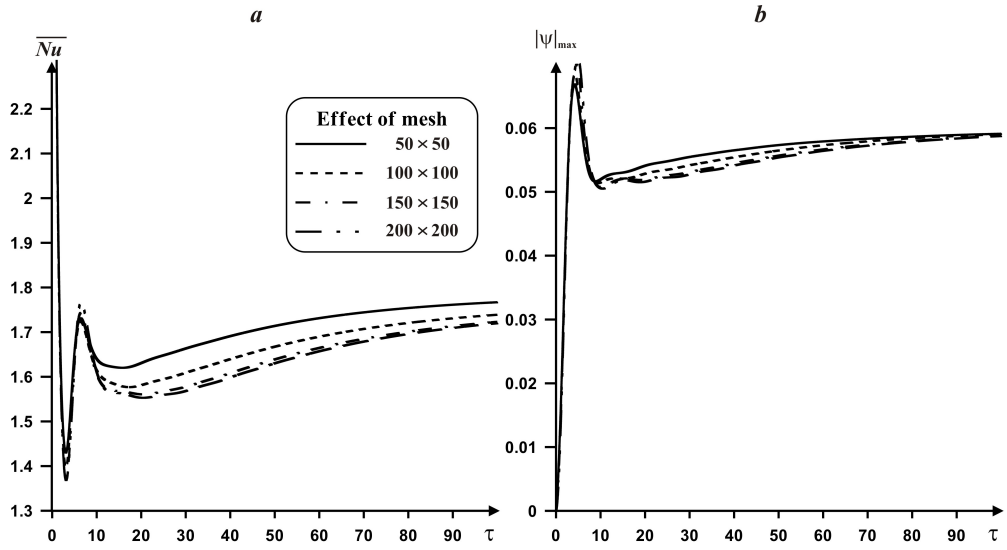

Fig. 2. Variation of $\overline{Nu}$ (left vertical wall) (*a*) and $|\psi|_{\max}$ (*b*) versus time and mesh parameters

On the basis of the conducted verifications the uniform grid of 150×150 points has been selected for the following analysis.

IV. Results and Discussion

Numerical analysis has been realized for the following values of key parameters: Rayleigh number ($Ra = 10^4$), Prandtl number ($Pr = 0.7$), Schmidt number ($Sc = 0.1$–100), buoyancy ratio parameter ($\beta = 0.0$–1.0), thermophoresis parameters ($N_T = 8$, $N_C = 2$), dimensionless thermophoretic coefficient ($k_T = 0.1$–1.0), undulation number ($\kappa = 0$–2), $a = 0.9$ and two cases of boundary conditions I – $T_1 = T_h$, $T_2 = T_c$, $C_1 = C_c$, $C_2 = C_h$ and II – $T_1 = T_c$, $T_2 = T_h$, $C_1 = C_h$, $C_2 = C_c$. Particular efforts have been focused on the effects of these parameters on the fluid flow, heat and mass transfer inside the wavy cavity. Streamlines, isotherms and isoconcentrations as well as average Nusselt and Sherwood numbers and fluid flow rate for different values of governing parameters mentioned above are illustrated in Figs. 3–14.

Figures 3 and 4 present distributions of streamlines, isotherms and isoconcentrations inside the wavy cavity in the case of different boundary conditions and for various values of Schmidt number. It should be noted that used boundary conditions reflect the effect of wavy wall on deposition and ablation of small particles at curved wall. The case of hot wavy wall and cold flat wall is demonstrated in Fig. 3. For $Sc = 0.1$ and $Sc = 1.0$ one can find a domination of heat and mass diffusion mechanism when isothermal and isoconcentrations are parallel to vertical walls of constant temperature and concentration. Moreover, taking into account the thermophoresis effect the small particles are distributed uniformly inside the cavity. An appearance of two convective cells of low intensity inside the cavity for these values of Schmidt number illustrates a formation of different temperature and concentration gradients within the cavity. Further increase in Schmidt number (Fig. 3*c*) leads to essential intensification of convective heat and mass transfer, where one major vortex is formed inside the cavity and three recirculations are at corners of the cavity. Isotherms illustrate more significant heating of the cavity upper part taking into account the major vortex shape, while recirculation in the upper wave trough reflects the formation of stagnant zone of high quasi-constant temperature. At the same time, low temperature disturbs from the right vertical wall along the bottom surface. Such a circulation defines a motion of small particles. Highest concentration is in the bottom right corner where a minor vortex circulates and lowest concentration is in the upper wave trough. It is worth noting that due to the thermophoresis effect the upper part has a low concentration of particles while the bottom part has a high concentration of particles.

In the case of hot flat vertical wall and cold wavy wall with the opposite distribution of concentration we have the fluid flow, heat and mass transfer patterns (Fig. 4) that are symmetry to the abovementioned. For low values of Schmidt number (Figs. 4*a* and *b*) the diffusion mechanism for heat and mass transfer is essential and location of convective cells cores as well as isotherms and isoconcentrations are opposite in comparison with Figs. 3*a* and *b*. When $Sc = 10$ (Figs. 4*c*) on can find also one major vortex and three minor ones. Highest particles concentration is inside the bottom wave

trough, while the lowest concentration in the upper right corner. The main reason for such behavior is the effect of thermophoresis force and geometry of the cavity with stagnation zones. It is interesting to note, that the considered mass buoyancy force has an opposite effect on the convection due to the temperature gradient for the considered case is directed in positive *x*-coordinate while the concentration gradient is directed in negative *x*-coordinate. But for the thermophoresis effect we have the particles circulation along the main circulation. If we consider the case when thermal Rayleigh number is equal to zero but concentration one is not zero the formed circulation will be opposite.

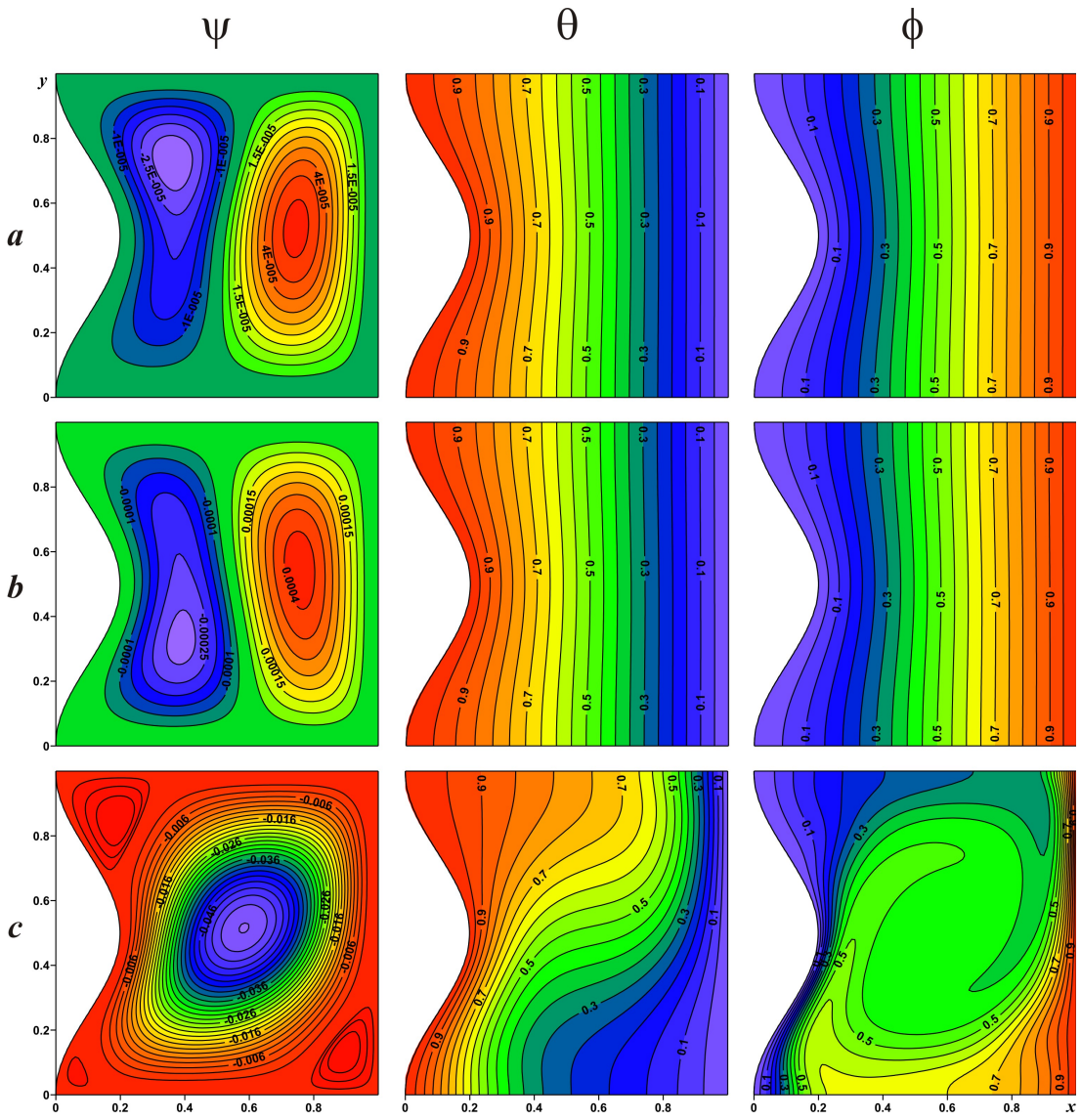

Fig. 3. Streamlines, isotherms and isoconcentrations (case I) for β=1.0, k_T=0.5, κ=1:

Sc=0.1 – *a*, *Sc*=1.0 – *b*, *Sc*=10.0 – *c*

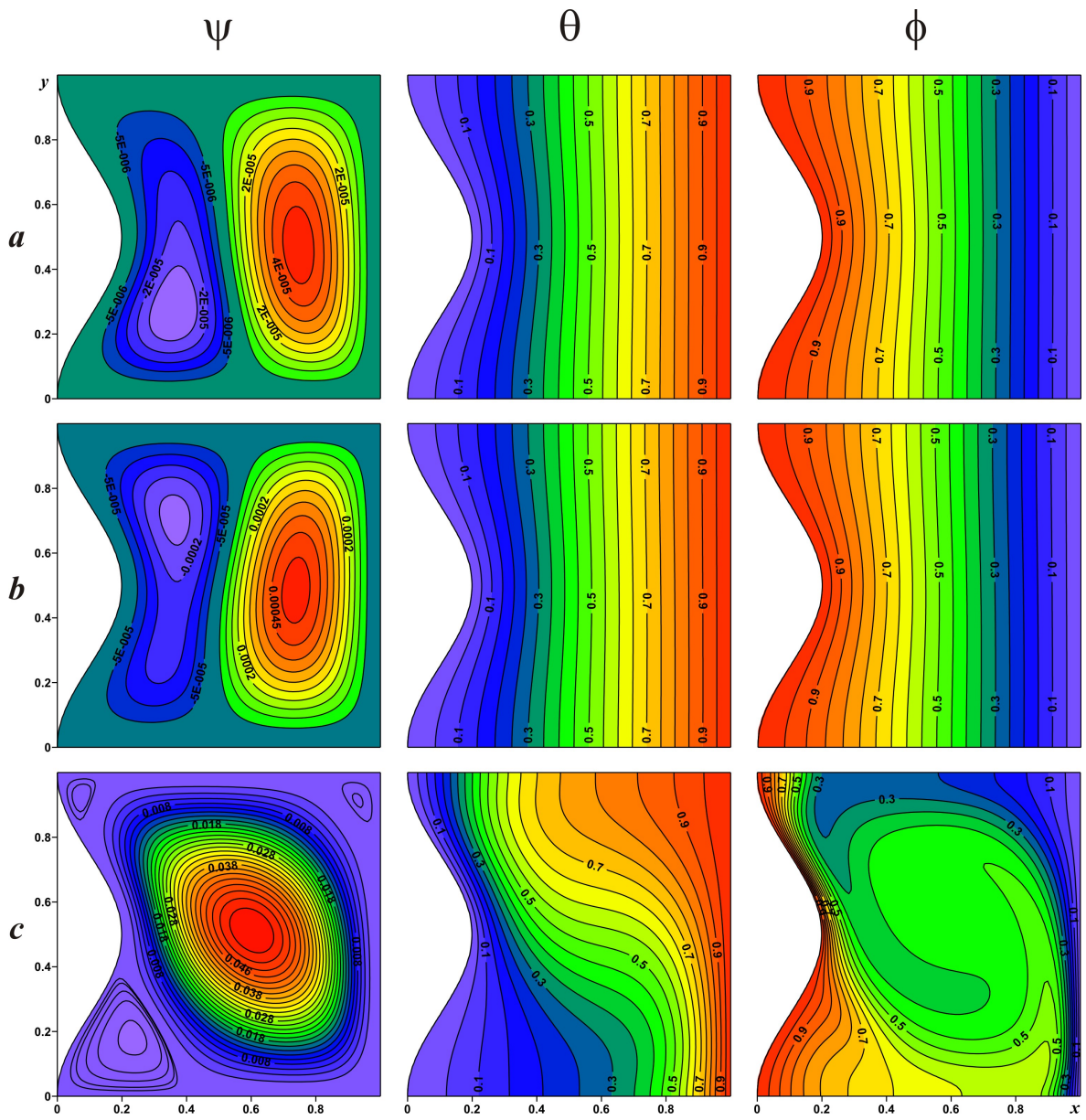

Fig. 4. Streamlines, isotherms and isoconcentrations (case II) for β=1.0, k_T=0.5, κ=1:

Sc=0.1 – *a*, Sc=1.0 – *b*, Sc=10.0 – *c*

The effects of Schmidt number and used boundary conditions on average Nusselt and Sherwood numbers at left wavy wall are presented in Fig. 5. As has been mentioned above, low values of Schmidt number reflect heat and mass conduction; therefore regardless of the considered boundary conditions these values are identical. An increase in Sc up to 10 leads to an essential growth of $\overline{Nu}$ and $\overline{Sh}$.

Average Nusselt number at $\tau = 200$ for different boundary conditions has identical values, while average Sherwood number does not obtain steady state value. The effect of dimensionless time is also interesting, namely, an increase in *Sc* leads to a growth of time needed for obtaining steady-state mode.

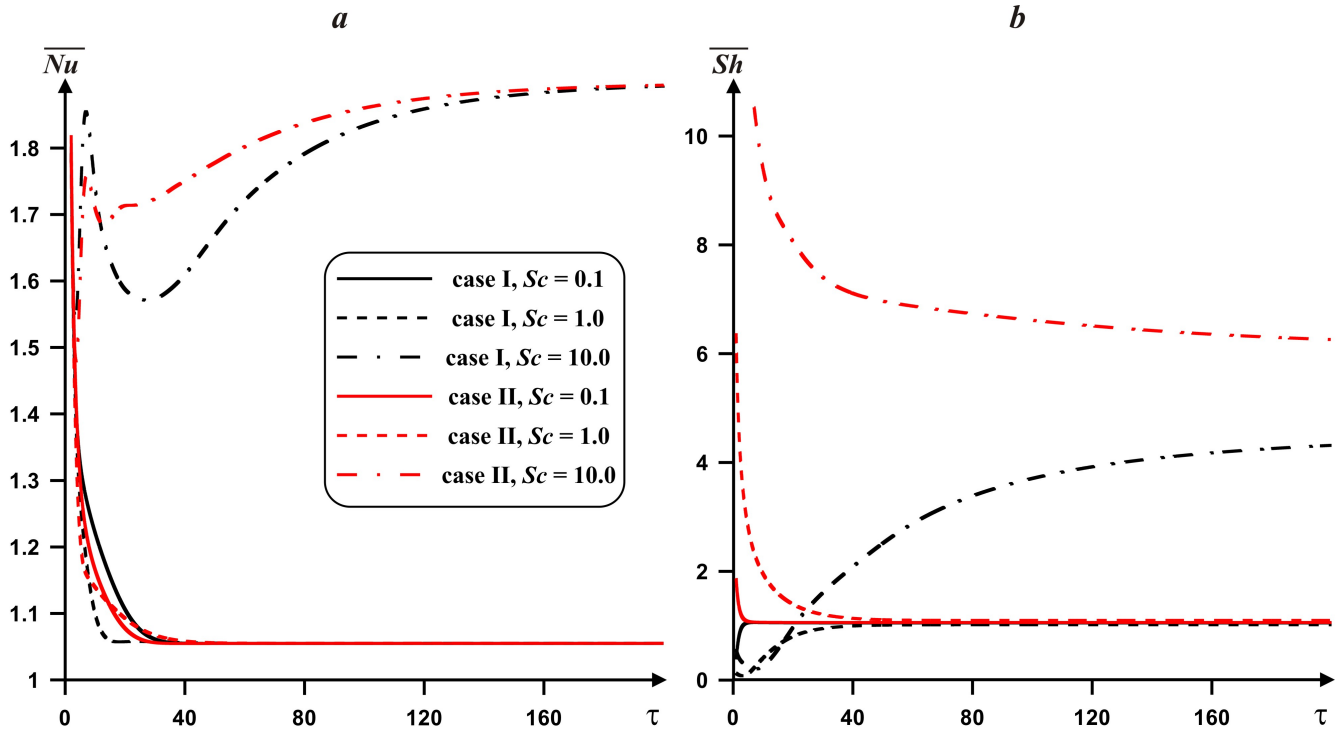

Fig. 5. Variations $\overline{Nu}$ (*a*) and $\overline{Sh}$ (*b*) at wavy wall for β=1.0, k_T=0.5, κ=1

Figures 6 and 7 show streamlines, isotherms and isoconcentrations for different values of buoyancy ratio parameter and used boundary conditions. Regardless of the analyzed case, an increase in β leads to a weak attenuation of the convective flow, heat transfer and mass transfer along the main vortex. More essential influence of mass flux reduces the heat transfer due to the opposite concentration effect as has been mentioned above that results in an appearance of addition recirculations in wave troughs and cavity corner. In the case of hot right wall and cold left one the effect of buoyancy ratio parameter is similar to the abovementioned.

Figure 8 demonstrates the heat and mass transfer enhancement with Schmidt number and the rate of this enhancement increases with the buoyancy ratio parameter. While average Nusselt and

Sherwood numbers decrease with a growth of β. It is worth noting that change of the analyzed boundary conditions leads to essential differences in average Sherwood number for high values of the buoyancy ratio parameter.

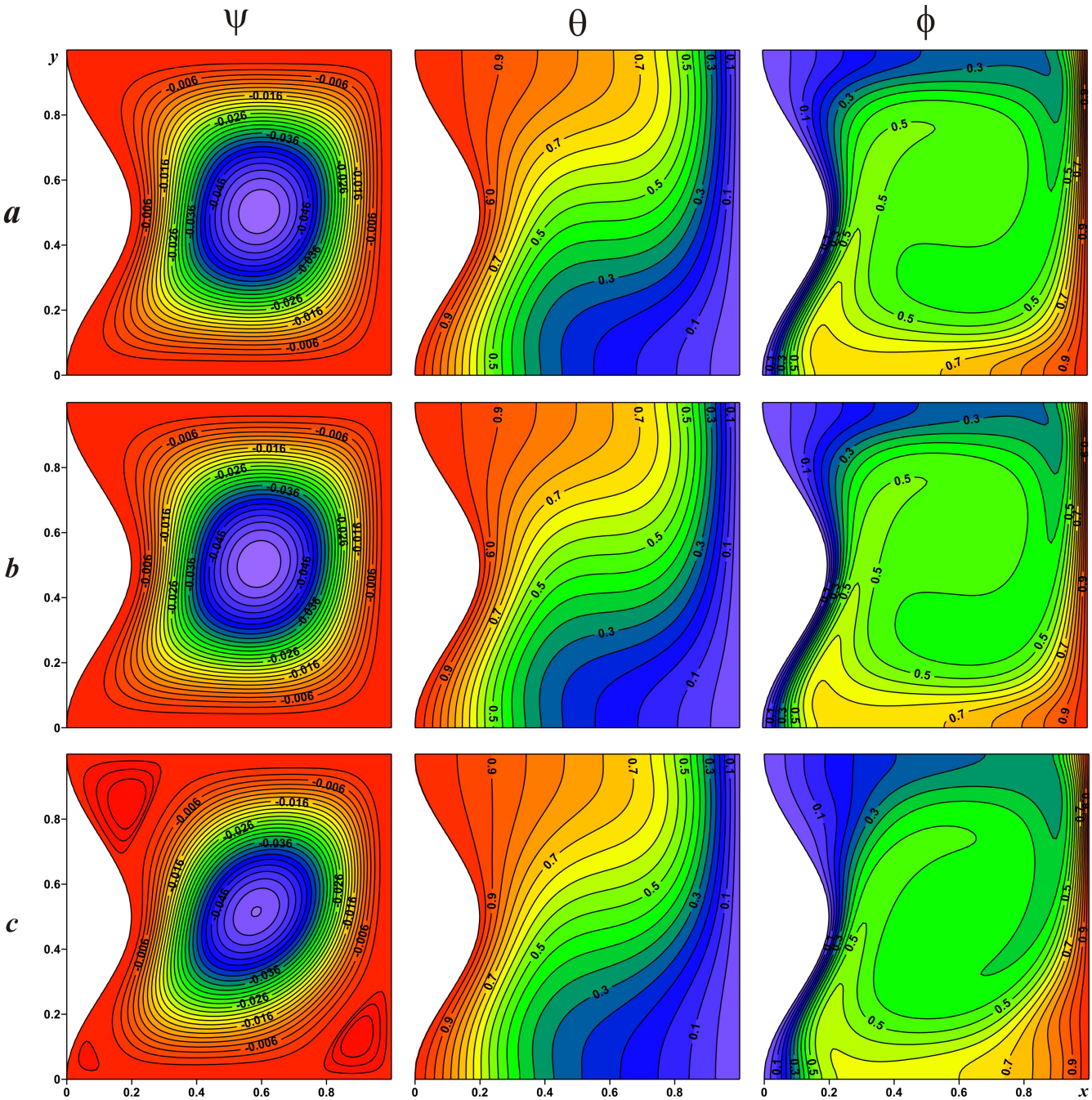

Fig. 6. Streamlines, isotherms and isoconcentrations (case I) for Sc=10.0, k_1=0.5, κ=1:

β=0.0 – *a*, β=0.1 – *b*, β=1.0 – *c*

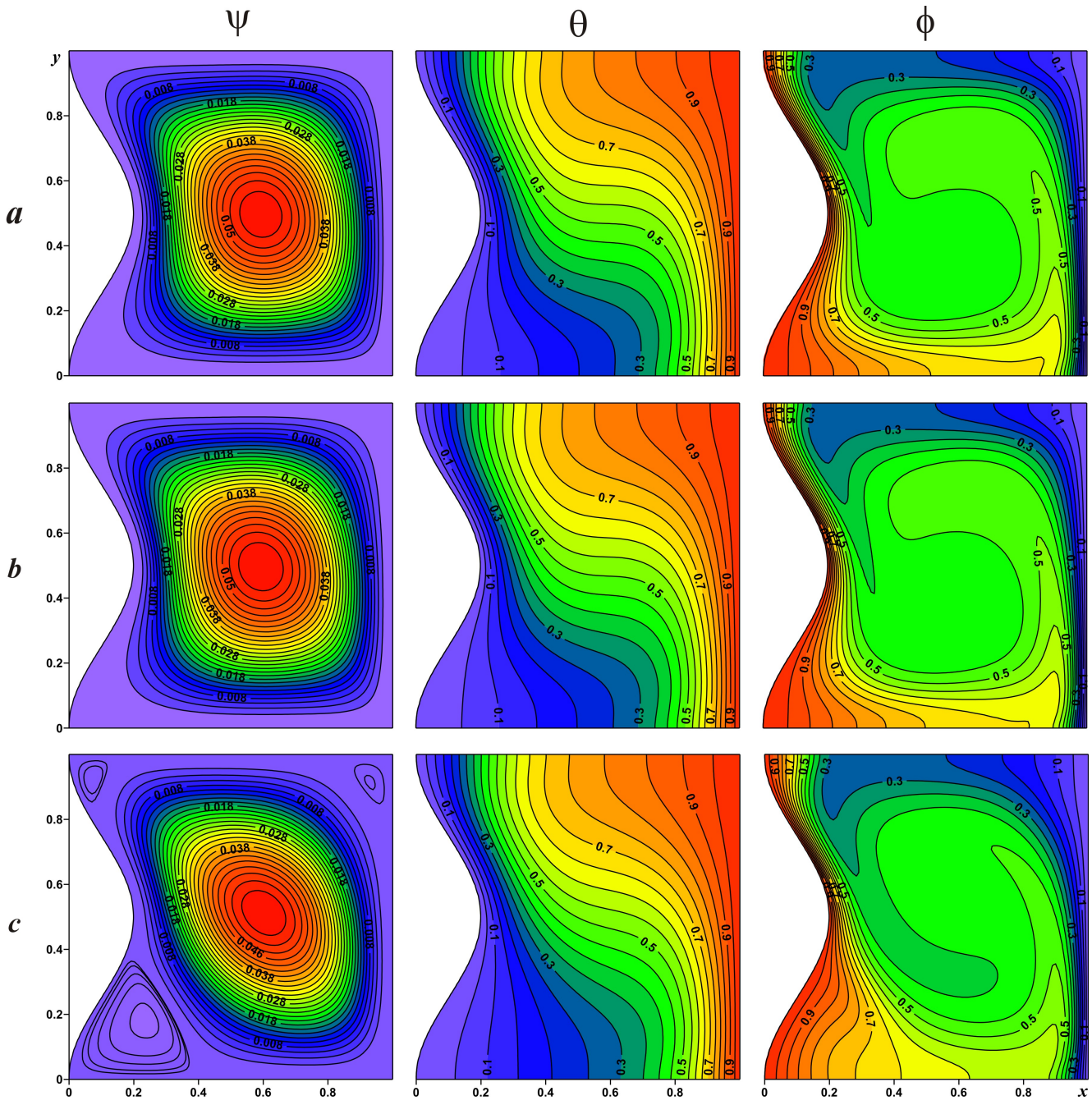

Fig. 7. Streamlines, isotherms and isoconcentrations (case II) for Sc=10.0, k_T=0.5, κ=1:

β=0.0 – *a*, β=0.1 – *b*, β=1.0 – *c*

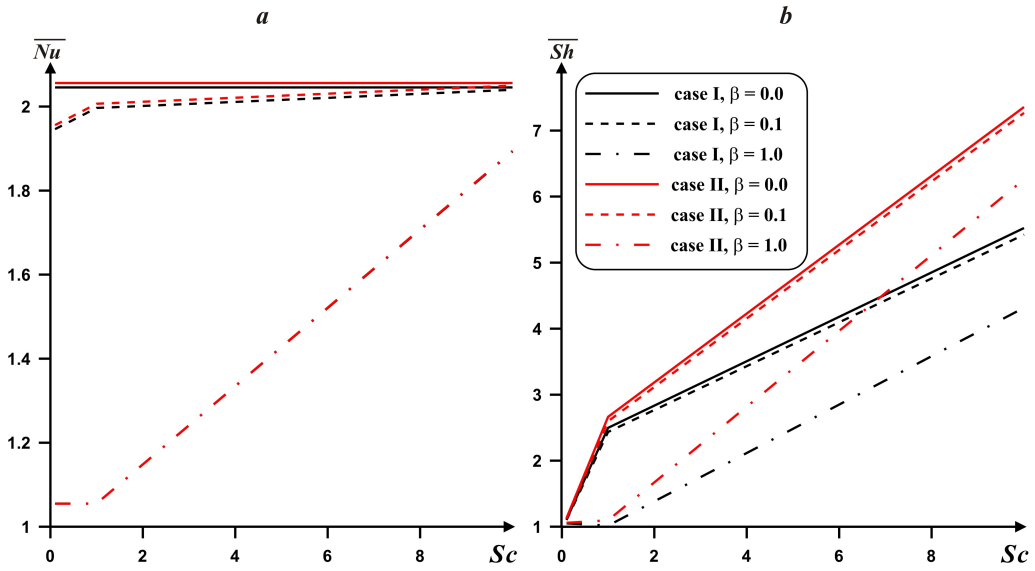

Fig. 8. Variations of $\overline{Nu}$ (*a*) and $\overline{Sh}$ (*b*) at wavy wall for k_T=0.5, κ=1

Figures 9–11 show the effect of dimensionless thermophoretic coefficient on fluid flow, heat and mass transfer patterns for $Sc = 10.0$, $\beta = 1.0$, $\kappa = 1$. Regardless of the analyzed boundary conditions, an increase in k_T leads to weak fluid flow intensification, while temperature field changes insignificantly and concentration field changes essentially. An increase in thermophoretic coefficient characterizes a growth of thermophoresis velocity (see Eq. (7)) that reflects an increase in particles concentration in the bottom right corner (Fig. 9) and left bottom wave trough (Fig. 10).

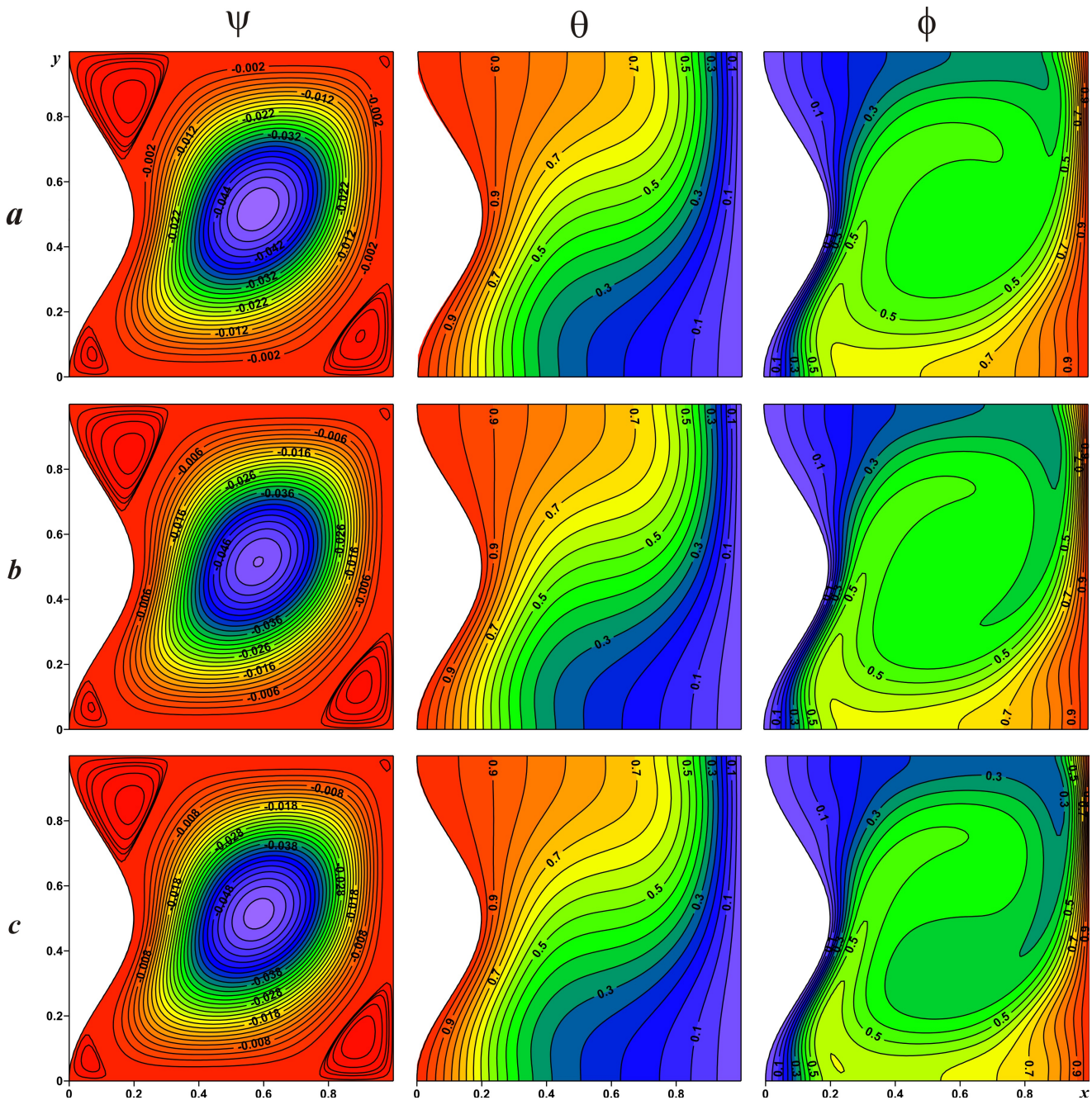

Fig. 9. Streamlines, isotherms and isoconcentrations (case I) for Sc=10.0, β=1.0, κ=1:

k_T=0.1 – *a*, k_T=0.5 – *b*, k_T=1.0 – *c*

Figure 11 presents the heat transfer enhancement with dimensionless thermophoretic coefficient and it is not dependent on the used boundary conditions. At the same time, this heat transfer intensification is more essential for high values of Schmidt number. In the case I average Sherwood

number is a weak decreasing function of k_T, while for the case II $\overline{Sh}$ is an increasing function of k_T. The main reason for such behavior is a growth of the surface length where particles subside.

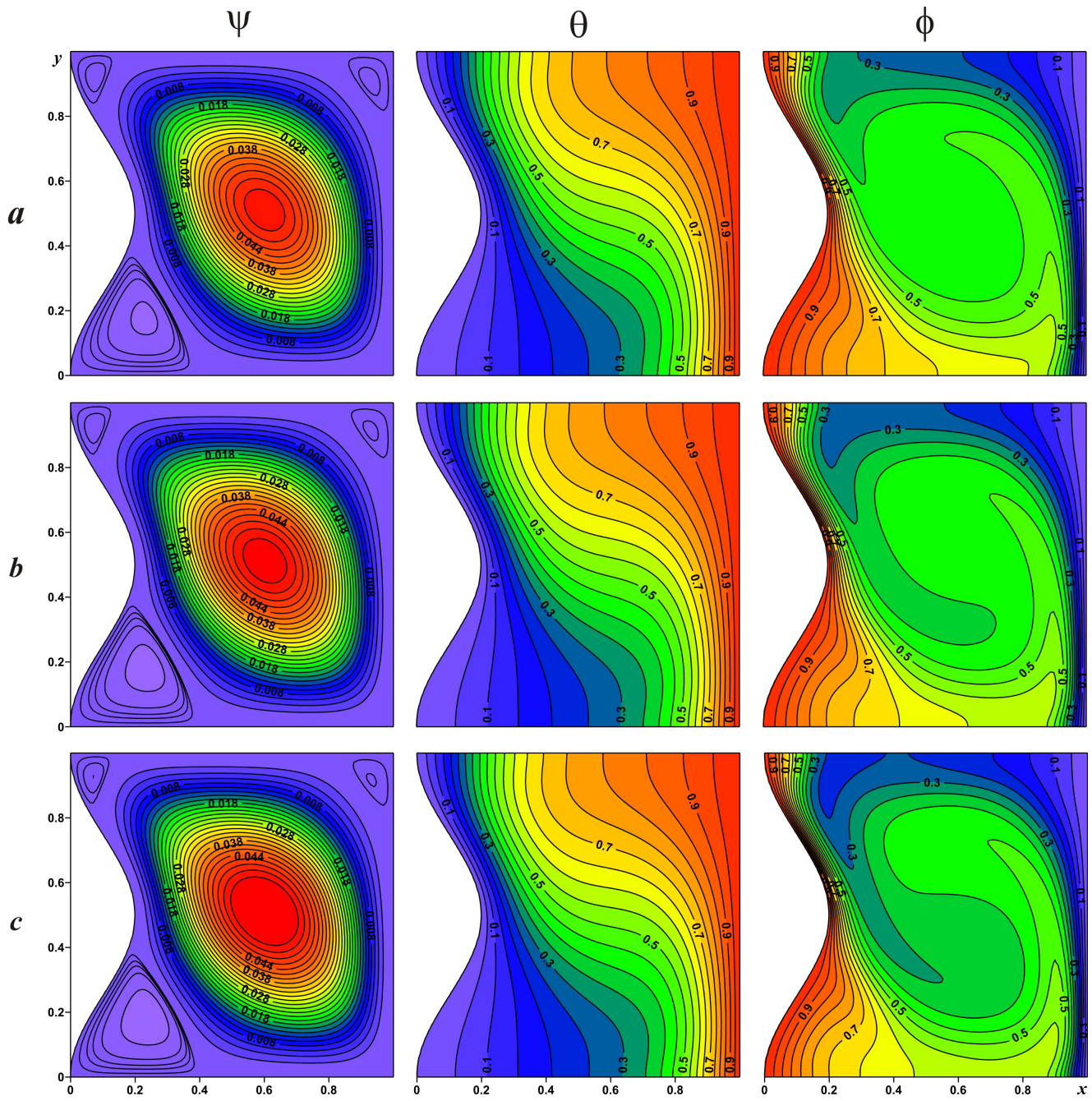

Fig. 10. Streamlines, isotherms and isoconcentrations (case II) for Sc=10.0, β=1.0, κ=1:

k_T=0.1 – *a*, k_T=0.5 – *b*, k_T=1.0 – *c*

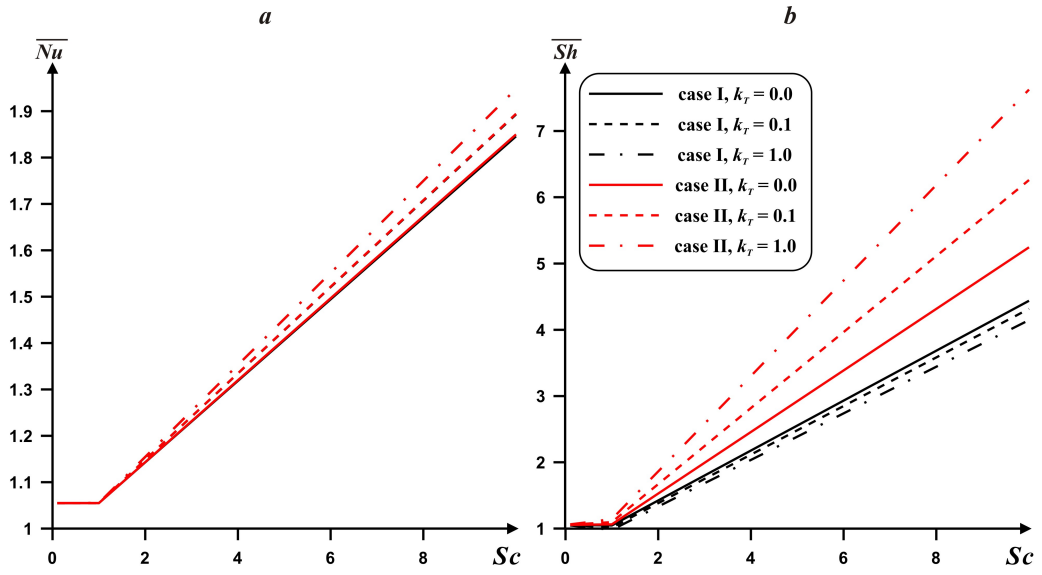

Fig. 11. Variations of $\overline{Nu}$ (*a*) and $\overline{Sh}$ (*b*) at wavy wall for β=1.0, κ=1

The effect of undulation number on streamlines, isotherms and isoconcentrations for different boundary conditions is presented in Figs. 12 and 13 for $Sc = 10.0$, $\beta = 1.0$, $k_T = 0.5$. Regardless of the used boundary conditions (cases I and II) the main reason for various flow, heat and mass transfer patterns is a deformation of internal fluid zone due to wave crests and troughs. For the considered range of κ we have the following analysis of fluid intensity: for the cases I and II $|\psi|_{\max}^{\kappa=0} = 0.062 > |\psi|_{\max}^{\kappa=2} = 0.057 > |\psi|_{\max}^{\kappa=1} = 0.054$. Therefore, the wave troughs define the fluid flow intensity. It should be noted that the value of undulation number does not change the location of zones with the highest and lowest values of particles concentration. One can find only the modification of the isoconcentrations and isotherms near the wavy wall.

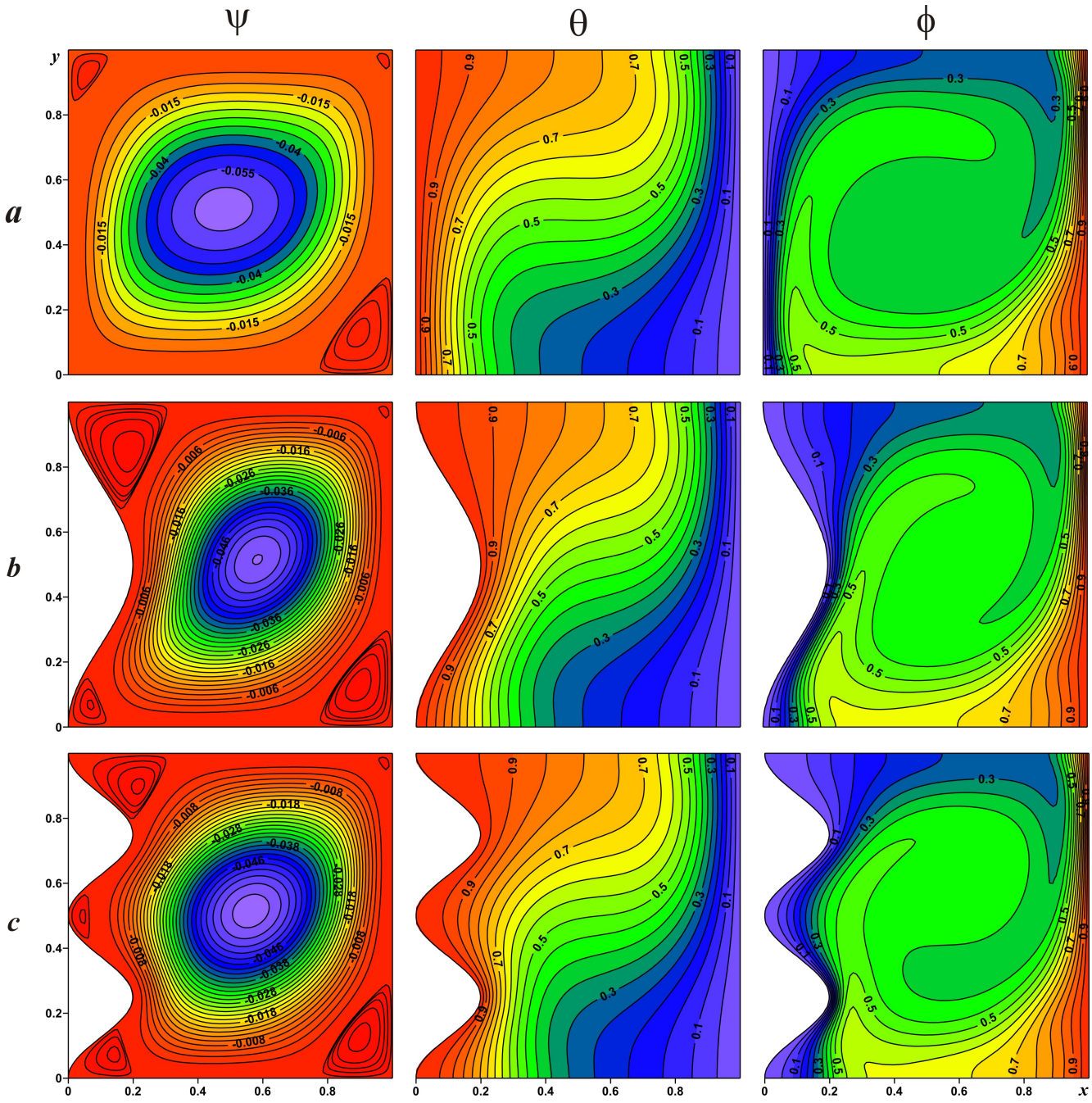

Fig. 12. Streamlines, isotherms and isoconcentrations (case I) for Sc=10.0, β=1.0, k_T=0.5:

κ=0 – *a*, κ=1 – *b*, κ=2 – *c*

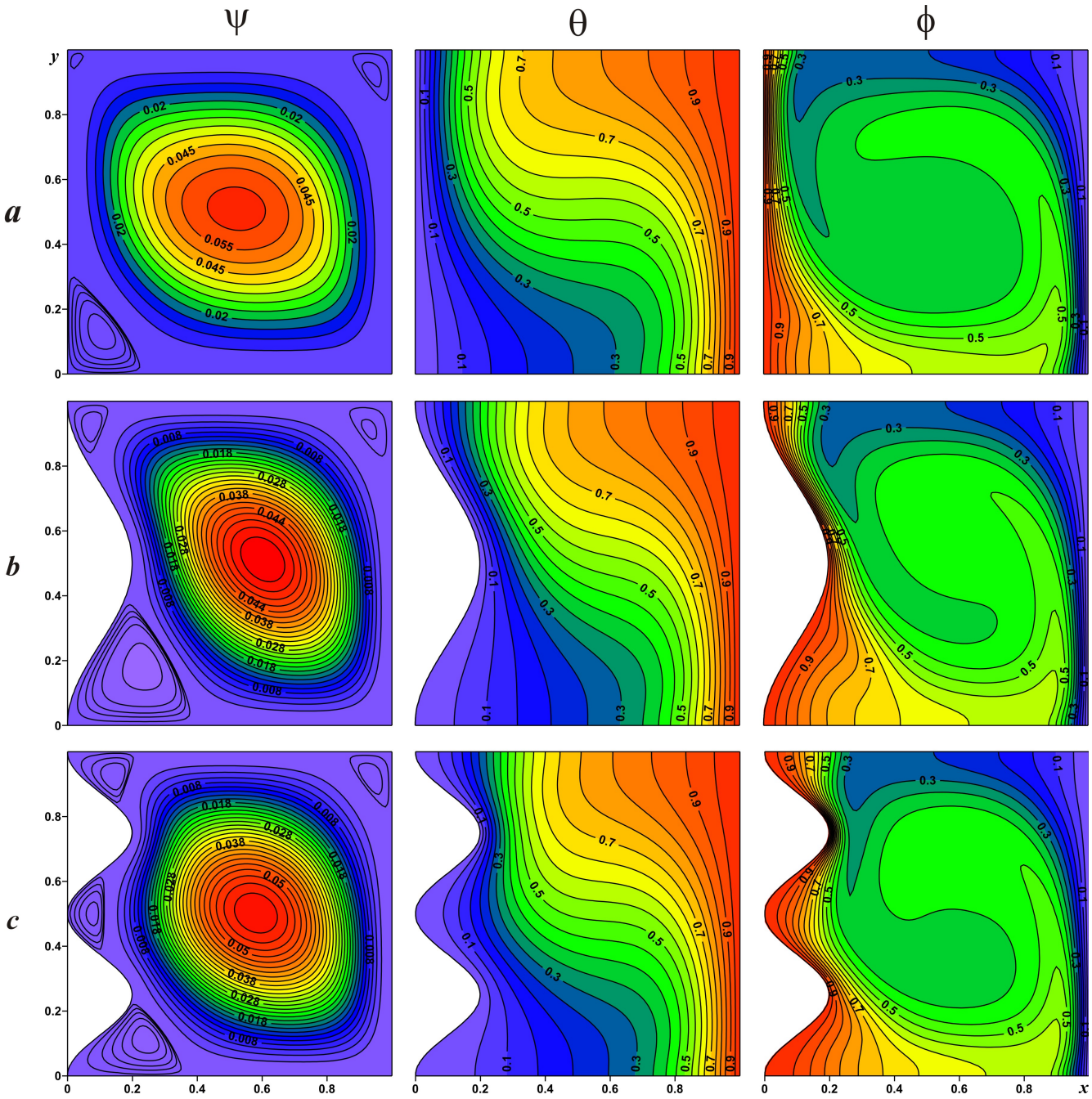

Fig. 13. Streamlines, isotherms and isoconcentrations (case II) for Sc=10.0, β=1.0, k_T=0.5:

κ=0 – *a*, κ=1 – *b*, κ=2 – *c*

The effect of undulation number on average Nusselt and Sherwood numbers at wavy wall for different boundary conditions is shown in Fig. 14. In the case of $Sc > 3$ a growth of undulation number leads to the heat transfer rate reduction regardless of the used boundary conditions (cases I and II). As

for average Sherwood number, an increase in κ for $Sc > 2$ also leads to a diminution of $\overline{Sh}$. While for $Sc < 2$ the dependences are non-linear. As has been mentioned above, in the case of the highest concentration along wavy wall average Sherwood number is greater in comparison with another considered case.

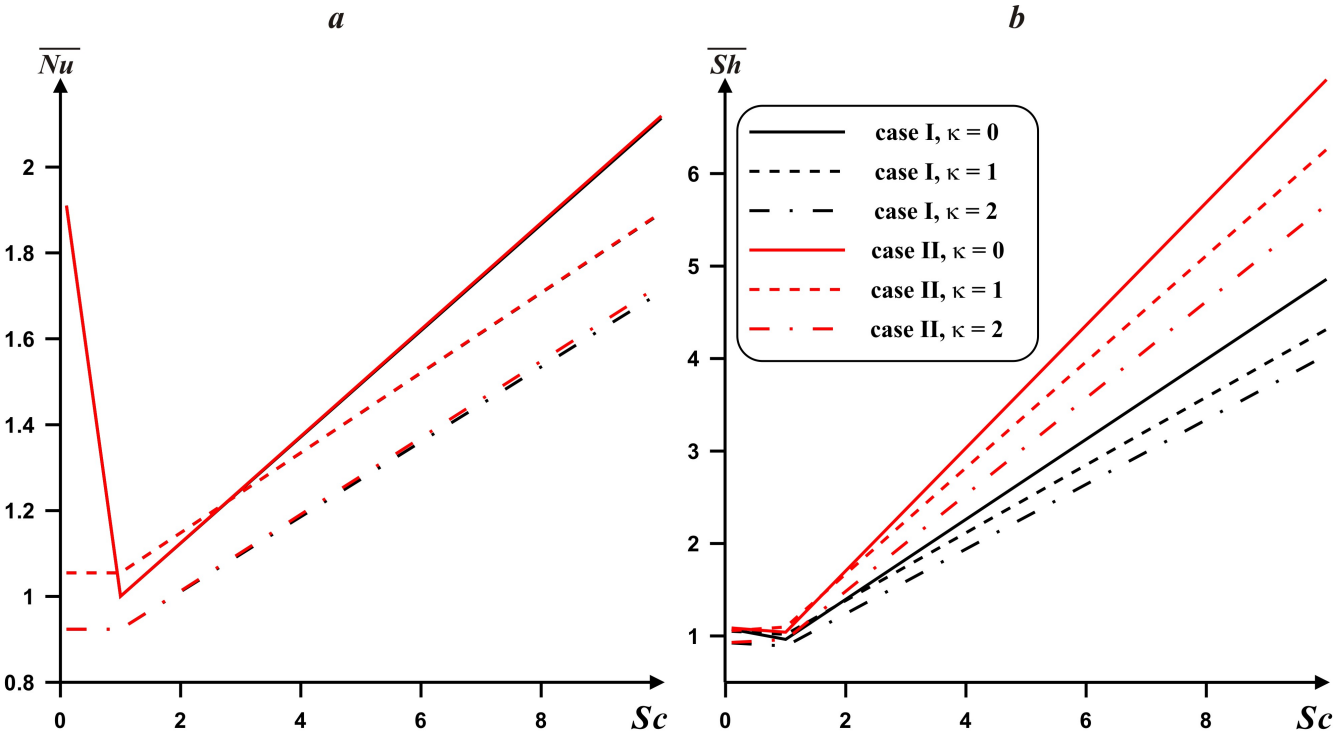

Fig. 14 Variations of $\overline{Nu}$ (*a*) and $\overline{Sh}$ (*b*) at wavy wall for β=1.0, k_T=0.5

V. Conclusions

In the present work we attempt to model natural convective flow in a wavy wall cavity considering the double-diffusion and thermophoresis effects. The initial domain was transformed using appropriate transformations in a rectangular one. The modified governing dimensionless partial differential equations were solved using a finite difference method of the second order accuracy. The flow characteristics such as streamlines, isotherms and isoconcentrations along with average Nusselt and Sherwood numbers at wavy wall were presented in graphical form for several values of the governing parameters. Two cases of differentially heated cavity were taken into account, namely: case I when left

wavy wall is kept at high temperature and low concentration, while the right wall is kept at low temperature and high concentration; case II when left wavy wall is kept at low temperature and high concentration, while the right wall is kept at high temperature and low concentration. The conducted analysis revealed that the average Nusselt number is an increasing function of Schmidt number and thermophoretic coefficient, and a decreasing function of buoyancy ratio parameter and undulation number for $Sc > 3$ regardless of the used boundary condition cases. At the same time, the average Sherwood number is an increasing function of Schmidt number and a thermophoretic coefficient for case II, and a decreasing function of buoyancy ratio parameter, undulation number for $Sc > 2$ and thermophoretic coefficient for case I. It should be noted that the waviness of the wall essentially affect the mass transfer taking into account the obtained results for the average Sherwood number.

Acknowledgements

This work of Mikhail A. Sheremet was supported by the Grants Council under the President of the Russian Federation (Project No. MD-2819.2017.8). The work of T. Grosan and I. Pop has been supported from the grant PN-III-P4-ID-PCE-2016-0036, UEFISCDI, Romania.

References

[1] Epstein, M., Hauser, G.M. and Henry, R.E., "Thermophoretic deposition of particles in natural convection flow from a vertical plate," *Journal of Heat Transfer*, Vol. 107, 1985, pp. 272–276. doi:10.1115/1.3247410

[2] Tsai, R. and Liang, L.J., "Correlation for thermophoretic deposition of aerosol particles onto cold plates," *Aerosol Science*, Vol. 32, 2001, pp. 473–487. doi.org/10.1016/S0021-8502(00)00095-1

[3] Jenson, F.J., Einset, E.O. and Fotiadis, D.I., "Flow phenomena in chemical vapor deposition of thin film," *Annual Review of Fluid Mechanics*, Vol. 23, 1991, pp. 197–232.

doi.org/10.1146/annurev.fl.23.010191.001213

[4] Opiolka, S., Schmidt, F. and Fissan, H., "Combined effect of electrophoresis and thermophoresis on particle deposition onto flat surfaces," *Journal of Aerosol Science*, Vol. 25, 1994, pp. 665–671.
doi.org/10.1016/0021-8502(94)90007-8

[5] Song, C.G. and Hwang, J., "Particle deposition on a rotating disk in application to vapor axial deposition (VAD) process," *Journal of Aerosol Science*, Vol. 29, 1988, pp. 99–114.
doi.org/10.1016/S0021-8502(97)00038-4

[6] Bakarov, S.P., "Thermophoresis in gas at small Knudsen numbers," *Aerosol Science and Technology*, Vol. 15, 1991, pp. 77–92.
doi.org/10.1080/02786829108959515

[7] He, C. and Ahmadi, G., "Particle deposition with thermophoresis in laminar and turbulent duct flow," *Aerosol Science and Technology*, Vol. 29, 1998, pp. 525–546.
doi.org/10.1080/02786829808965588

[8] Piazza, R. and Parola, A., "Thermophoresis in colloidal suspensions," *Journal Physics Condensed Matter* 20 (2008) 153102.
doi:10.1088/0953-8984/20/15/153102

[9] Goren, S.L., "Thermophoresis of aerosol particles in the laminar boundary layer on a flat plate," *Journal Colloid Interface Science*, Vol. 61, 1977, pp. 77–85.
doi.org/10.1016/0021-9797(77)90416-7

[10] Wang, C.-C. and Chen, C.-K., "Thermophoresis deposition of particles from a boundary layer flow onto a continuously moving wavy surface," *Acta Mechanica*, Vol. 181, 2006, pp. 139–151.
doi: 10.1007/s00707-005-0297-0

[11] Chamka, A.J. and Pop, I., "Effect of thermophoresis particle deposition in free convection boundary layer from a vertical flat plate embedded in a porous medium," *International*

Communication in Heat and Mass Transfer, Vol. 31, 2004, pp. 421–430.
doi.org/10.1016/j.icheatmasstransfer.2004.02.012

[12] Postelnicu, A., "Effects of thermophoresis particle deposition in free convection boundary layer from a horizontal flat plate embedded in a porous medium," *International Journal of Heat and Mass Transfer*, Vol. 50, 2007, pp. 2981–2985.
doi.org/10.1016/j.ijheatmasstransfer.2006.12.012

[13] Bejan, A., Convection Heat Transfer (3rd edition), John Wiley & Sons, New York, 2004

[14] De Vahl Davis, G., "Natural convection of air in a square cavity: a benchmark numerical solution," *International Journal of Numerical Methods in Fluids*, Vol. 2, 1983, pp. 249–264.
doi: 10.1002/fld.1650030305

[15] Beghein, C., Haghighat, F. and Allard, F., "Numerical study of double-diffusive natural convection in a square cavity," *International Journal of Heat and Mass Transfer*, Vol. 35, 1992, pp. 833–846
doi.org/10.1016/0017-9310(92)90251-M

[16] Sheremet, M.A., "The influence of cross effects on the characteristics of heat and mass transfer in the conditions of conjugate natural convection," *Journal of Engineering Thermophysics*, Vol. 19, 2010, pp. 119–127.
doi: 10.1134/S1810232810030021

[17] Sezai, I. and Mohamad, A.A., "Double-diffusive convection in a cubic enclosure with opposing temperature and concentration gradients," *Physics of Fluids*, Vol. 12, 2000, pp. 2210–2223.
doi.org/10.1063/1.1286422

[18] Kuznetsov, G.V. and Sheremet, M.A., "Conjugate heat transfer in an enclosure under the condition of internal mass transfer and in the presence of the local heat source," *International Journal of Heat and Mass Transfer*, Vol. 52, 2009, pp. 1–8.
doi.org/10.1016/j.ijheatmasstransfer.2008.06.034

[19] Kuznetsov, G.V. and Sheremet, M.A., "A numerical simulation of double-diffusive conjugate natural convection in an enclosure," *International Journal of Thermal Sciences*, Vol. 50, 2011, pp. 1878–1886.
doi.org/10.1016/j.ijthermalsci.2011.05.003

[20] Weinberg, M.C., "Thermophoretic deposition of particles in laminar flow in a concentric annulus," *Journal American Ceramic Society*, Vol. 66, 1983, pp. 439–445.
doi: 10.1111/j.1151-2916.1983.tb10077.x

[21] Fiebig, M., Hilgenstock, M. and Riemann, H.-A., "The modified chemical vapour deposition process in a concentric annulus," *Aerosol Science Technology*, Vol. 9, 1988, pp. 237–249.
doi.org/10.1080/02786828808959211

[22] Grosan, T., Pop, R. and Pop, I., "Thermophoretic deposition of particles in fully developed mixed convection flow in a parallel-plate vertical channel," *Heat and Mass Transfer*, Vol. 45, 2009, pp. 503–509.
dx.doi.org/10.1007/s00231-009-0568-8

[23] Chang, Y.C., Ranade (Arun), M.B. and Gentry, J.W., "Thermophoretic deposition in flow along an annular cross-section: experiment and simulation," *Journal of Aerosol Science*, Vol. 26, 1995, pp. 407–428.
doi.org/10.1016/0021-8502(94)00118-I

[24] Chein, R. and Liao, W., "Thermophoretic effects on nano-particle deposition in channel flow," *Heat and Mass Transfer*, Vol. 42, 2005, pp. 71–79.
doi: 10.1007/s00231-005-0662-5

[25] Talbot, L., Cheng, R.K., Schefer, A.W. and Willis, D.R., "Thermophoresis of particles in a heated boundary layer," *Journal of Fluid Mechanics*, Vol. 101, 1980, pp. 737–758.
doi.org/10.1017/S0022112080001905

[26] Batchelor, G.K. and Shen, C., "Thermophoretic deposition in gas flow over cold surfaces,"

Journal of Colloid Interface Science, Vol. 107, 1985, pp. 21–37.

doi.org/10.1016/0021-9797(85)90145-6

[27] Sogard, M., "Methods and devices for hybridization and binding assays using thermophoresis," Patent US 8852858 B2, 2014.

[28] Komiyama, H., "Process for preparation of ceramic film," Patent US 4654228 A, 1987.

[29] Varol, Y. and Oztop, H.F., "Free convection in a shallow wavy enclosure," *International Communication in Heat and Mass Transfer*, Vol. 33, 2006, pp. 764–771.

doi.org/10.1016/j.icheatmasstransfer.2006.02.004

[30] Sultana, Z. and Hyder, Md.N., "Non-Darcy free convection inside a wavy enclosure," *International Communication in Heat and Mass Transfer*, Vol. 34, 2007, pp. 136–146.

doi.org/10.1016/j.icheatmasstransfer.2006.10.007

[31] Shenoy, A., Sheremet, M.A. and Pop, I., "Flow and Heat Transfer past Wavy Surfaces: Viscous Fluids, Porous Media and Nanofluids," *CRC Press, Taylor & Francis Group*, New York, 2016.

[32] Ridouane, E.H. and Campo, A., "Free convection performance of circular cavities having two active curved vertical sides and two inactive curved horizontal sides," *Applied Thermal Engineering*, Vol. 26, 2006, pp. 2409–2416.

doi.org/10.1016/j.applthermaleng.2006.02.019

[33] Siddiqa, S., Abrar, M.N., Hossain, M.A. and Awais, M., "Dynamics of two-phase dusty fluid flow along a wavy surface," *International Journal of Nonlinear Sciences and Numerical Simulation*, Vol. 17, 2016, pp.185-193.

DOI 10.1515/ijnsns-2015-0044

[34] Siddiqa, S., Abra, M.N., Hossain, M.A. and Gorla, R.S.R., "Double diffusive natural convection flow over a wavy surface situated in a non-absorbing medium," *International Journal of Heat and Mass Transfer*, Vol. 109, 2017, pp. 200-208.
doi.org/10.1016/j.ijheatmasstransfer.2017.01.087

[35] Mahajan, R.L. and Angirasa, D., "Combined heat and mass transfer by natural convection with

opposing buoyancies," *ASME Journal of Heat Transfer*, Vol. 115, 1993, pp. 606–612. doi:10.1115/1.2910730